

## EFFECTS OF BROWNIAN MOTION ON FREEZING OF PCM CONTAINING NANOPARTICLES

by

**M. Y. ABDOLLAHZADEH JAMALABADI<sup>a,b</sup> and Jae Hyun PARK<sup>c\*</sup>**

<sup>a</sup> Maritime University of Chabahar, Chabahar, Iran

<sup>b</sup> Graduate School of Mechanical and Aerospace Engineering,  
Gyeongsang National University, Jinju, South Korea

<sup>c</sup> Department of Aerospace and System Engineering,  
Research Center for Aircraft Parts Technology,  
Gyeongsang National University, Jinju, South Korea

Original scientific paper

DOI:10.2298/TSCI140413094A

*Enhancement of thermal and heat transfer capabilities of phase change materials with addition of nanoparticles is reported. The mixed nanofluid of phase change material and nanoparticles presents a high thermal conductivity and low heat capacity and latent heat, in comparison with the base fluid. In order to present the thermophysical effects of nanoparticles, a solidification of nanofluid in a rectangular enclosure with natural convection induced by different wall temperatures is considered. The results show that the balance between the solidification acceleration by nanoparticles and slowing-down by phase change material gives rise to control the medium temperature. It indicates that this kind of mixture has great potential in various applications which requires temperature regulation. Also, the Brownian motion of nanoparticles enhances the convective heat transfer much more than the conductive transfer.*

Key words: *nanoparticles, nanofluids, phase change, temperature control, natural convection, solidification, Brownian motion*

### Introduction

Phase change materials (PCM) are used to control the temperatures in diverse industrial applications including in electronic industries, communication systems, power plant boilers, greenhouse heating systems, thermal management of buildings, etc [1, 2]. During the heat transfer with phase change, the energy is stored in the form of latent heat. The present nanotechnology-based improvement of material properties provides us a great chance for new technological innovations in many fields of engineering [3-5]. The enhancement thermal conductivity of fluid by adding fine particles is first proposed by Maxwell [6]. With the rapid progress of nanotechnology, the nanometer-sized metal or metal oxide particles (smaller than 100 nm) are able to introduce to a single-phase base fluid to form the resulting *nanofluid* mixture and the thermal conductivities of the nanofluids are significantly increased over their base fluids [7, 8]. The other thermophysical properties of nanoparticle embedded PCM have been also extensively studied [9]. Khodadadi and Hosseinizadeh [10] have investigated the thermal behavior of nanoenhanced phase change material (NEPCM) in square cavity. In their study, the

\* Corresponding author; e-mail: parkj@gnu.ac.kr

thermophysical effect of nanoparticle is assumed constant. Ranjbar *et al.* [11] reported the heat transfer enhancement in the latent heat thermal energy storage system through dispersion of nanoparticle. Valan Arasu *et al.* [12] have carried out a numerical analysis of the performance enhancement of paraffin wax with nanoalumina ( $\text{Al}_2\text{O}_3$ ) particles in comparison with simple paraffin wax in a concentric double pipe heat exchanger. To our best knowledge, the effects of Brownian motion on the freezing of nanofluids have not been discussed yet [13, 14].

The purpose of this paper is to investigate the effects of Brownian motion of nanoparticles on the freezing of the mixture of nanoparticle and PCM in a square cavity with temperature gradient. In the present study, the properties of the PCM with nanoparticles vary during the phase change and the Brownian motion of nanoparticles is also included.

### Problem statement

The schematic of the problem is illustrated in fig. 1. The cavity is filled with nanofluid that is a mixture of an inorganic hydrated salt TH29 PCM [15] and solid copper nanoparticles. The TH29, made by TEAP Energy (<http://www.teappcm.com>), is an inorganic PCM composed primarily of calcium chloride hexahydrate ( $\text{CaCl}_2 \cdot 6\text{H}_2\text{O}$ ) with unknown (proprietary) additives [16]. With different wall temperatures, an unsteady buoyancy-driven convective flow accompanying with phase change is formed in the cavity. Three particle volume fractions of 0, 0.1 and 0.2 are considered. The associated thermophysical properties of PCM, nanoparticle and nanofluid are given in Table 1.

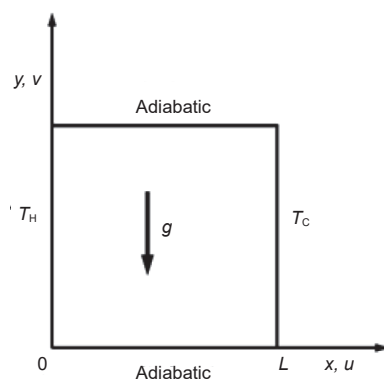


Figure 1. Schematic of the system

change problem including solidification, the previous studies have reported that the theoretical results using the simple Newtonian model are in good agreement with the experimental data [17-19]. Hence, the Newtonian model was employed in the present study; (2) Thermophysical properties of the nanofluid are constant; (3) buoyancy force is modeled with Boussinesq approximation; (4) The base fluid and the solid nanoparticles are in thermal equilibrium.

### Governing equations

In this study, the following assumptions are used: (1) the nanofluid is an incompressible Newtonian fluid. A nanofluid can be modeled as either Newtonian or non-Newtonian fluid. Fortunately, this kind of phase

Table 1. Thermophysical properties of base fluid, nanoparticle and nanofluid [10]

	PCM		Copper nanoparticle	$\phi = 0.1$		$\phi = 0.2$	
	liquid	solid	solid	liquid	solid	liquid	solid
$\rho$	1530	1710	8954	2434.4	2272.4	3014.8	3158.8
$k$	0.53	1.09	400	0.8	1.45	0.98	1.63
$c_p$	2200	1400	383	1503.3	1010.07	1140.3	806.9
$\beta$	$2 \cdot 10^{-4}$	–	$1.67 \cdot 10^{-5}$	$6.8 \cdot 10^{-5}$	–	$5.1 \cdot 10^{-5}$	–
$H_{sf}$	187000		–	115303.58	–	77947	–
$\mu$	0.00533		–	$7.3 \cdot 10^{-3}$	–	$1.16 \cdot 10^{-2}$	–

Then, the two-dimensional unsteady momentum conservation equations for this problem are expressed as:

– continuity

$$\frac{\partial \rho}{\partial t} + \frac{\partial \rho u}{\partial x} + \frac{\partial \rho v}{\partial y} = 0 \quad (1)$$

– x-momentum equation

$$\frac{\partial u}{\partial t} + u \frac{\partial u}{\partial x} + v \frac{\partial u}{\partial y} = \frac{1}{\rho_{nf}} \frac{\partial p}{\partial x} + \nu_{nf} \nabla^2 u \quad (2)$$

– y-momentum equation

$$\frac{\partial v}{\partial t} + u \frac{\partial v}{\partial x} + v \frac{\partial v}{\partial y} = \frac{1}{\rho_{nf}} \frac{\partial p}{\partial y} + \nu_{nf} \nabla^2 v - \beta_{nf} g (T - T_{ref}) \quad (3)$$

The effective properties of nanofluid such as density, heat capacity, etc., are modeled with a following simple relation [11, 20]:

$$\rho_{nf} = (1 - \phi) \rho_f + \phi \rho_s \quad (4)$$

$$(\rho c_p)_{nf} = (1 - \phi) (\rho c_p)_f + \phi (\rho c_p)_s \quad (5)$$

$$(\rho \beta)_{nf} = (1 - \phi) (\rho \beta)_f + \phi (\rho \beta)_s \quad (6)$$

The density variation due to phase change makes this problem complicated. In this paper, gas release and pressure increase during the solidification was neglected. Also, the latent heat of nanofluid is modeled as [11, 20]:

$$(\rho H_{sf})_{nf} = (1 - \phi) (\rho H_{sf})_f \quad (8)$$

Batchelor [21] derived a general viscosity relation for solid particle suspensions by adding to the Brownian effect to the original Einstein formulation for infinitely dilute case [22, 23]:

$$\mu_{nf} = \mu_f (1 + 2.5\phi + 6.2\phi^2) \quad (7)$$

where the linear term is due to Einstein [24]. The term with  $\phi^2$  presents the co-operative effects of the hydrodynamic interactions of pairs of spheres and the Brownian motion. Also, Prasher et al. [25] proposed the thermal conductivity for nanofluid by using the Maxwell-Garnett model [26] and the Nusselt number correlation for particle-to-fluid heat transfer in fluidized beds [27]:

$$\frac{k_{nf}}{k_f} = \frac{k_s + 2k_f - 2\phi(k_f - k_s)}{k_s + 2k_f + \phi(k_f - k_s)} \left[ 1 + A (\text{Re}_p)^m \text{Pr}^{0.333} \phi \right] \quad (9)$$

In this expression,  $\text{Re}_p$  is the particle Reynolds number based on Brownian velocity, which is defined as:

$$\text{Re}_p = \frac{1}{\nu_f} \sqrt{\frac{18k_B T}{\pi \rho_p d_p}}$$

where  $\nu_f$  is the kinematic viscosity of base fluid,  $\rho_p$  – the particle density,  $d_p$  – the particle diameter,  $T$  – the medium temperature,  $k_B$  – the Boltzmann constant ( $1.38 \cdot 10^{-23}$  J/K). The Prandtl number  $Pr = (C_{p,f} \mu_f) / k_f$  in eq. (9) is the value for base fluid. Khodadai and Hosseinizadeh [10] employed the Maxwell-Garnett model expressed as the formula without the parenthesis part of eq. (9) to the study of nanoparticle-enhanced phase change material (NEPCM) whose volume fraction is in the range of 10-20%. Advanced from this, we used eq. (9) to include the Brownian motion of particles as well. The particles used in this study have the size of 10 nm ( $Re_p = 1.87 \cdot 10^{-2}$ ), and the constants in eq. (9) are  $A = 40000$  and  $m = 2.75$ .

The unsteady energy conservation equation for this problem is:

$$\frac{\partial H}{\partial t} + \frac{\partial}{\partial x}(uH) + \frac{\partial}{\partial y}(vH) = \frac{\partial}{\partial x}\left(k \frac{\partial T}{\partial x}\right) + \frac{\partial}{\partial y}\left(k \frac{\partial T}{\partial y}\right) \quad (10)$$

where the enthalpy  $H$  varies depending on the phase:

$$H_{\text{solid}} = \rho_s C_{p,s} (T - T_{\text{ref}}) \quad \text{for} \quad T < T_m \quad (11)$$

$$H_{\text{liquid}} = \rho_l C_{p,l} (T - T_m) + H_{\text{sf}} + H_{\text{solid}}(T_m) \quad \text{for} \quad T > T_m \quad (12)$$

with the phase change temperature of  $T_m$ . The liquid fraction (ratio of PCM enthalpy to liquid enthalpy)  $\gamma$  can be defined on the isotherm with  $T = T_m$ :

$$\gamma = \frac{H_{\text{liquid}} - H_{\text{solid}}(T_m)}{H_{\text{sf}}} \quad (13)$$

Throughout the simulation, the temperature difference between the two walls is maintained as  $\Delta T = 10$  K as  $T_m = T_H$  and  $T_C = T_m - \Delta T$ . The other boundary conditions are:

$$u = v = \frac{\partial T}{\partial y} = 0 \quad \text{at} \quad y = 0, L \quad \text{and} \quad 0 \leq x \leq L \quad (14)$$

$$u = v = 0, \quad T = T_H \quad \text{at} \quad x = 0 \quad \text{and} \quad 0 \leq y \leq L \quad (15)$$

$$u = v = 0, \quad T = T_C \quad \text{at} \quad x = L \quad \text{and} \quad 0 \leq y \leq L \quad (16)$$

Initially, the temperatures of both left and right walls are equal as  $T = T_m$  and at  $t = 0$  the temperature of the right wall is suddenly lowered at 3 K below the freezing temperature  $T_m$  of the base fluid. After a fluid flow is fully developed under this conditions, then the temperature of right wall is cooled again as  $T_C = T_m - \Delta T$ . Advanced from [10] assuming that the fully-developed natural convection for  $t < 0$ , this study considers the realistic natural convection profiles as an initial condition for the phase change in enclosure. At  $t = 0$ , the PCM on the right side starts to freeze, the solid front travels to the left, and the remainder of the cavity that is a liquid will experience natural convection.

## Numerical procedure

The SIMPLE method [28] was employed with modified QUICK differencing scheme [29]. In order to avoid pressure fluctuations in the pressure correction equation, the Rhie-Chaw method was used [30]. The relaxation factors for the velocity components, pressure correction, thermal energy, and liquid fraction were 0.5, 0.3, 1, and 0.9, respectively. Time discret-

ization was handled with the implicit Euler method. The time step was chosen to satisfy the Courant–Friedrichs–Lewy condition (CFL condition). All the simulations in this paper have been performed with FLUENT 6.1 [31]. The solution was judged as being converged when all the maximum residuals of variables are less than  $10^{-7}$  except for temperature whose criterion of  $10^{-9}$ . At each time step, about 500 iterations are required for convergence.

### Results and discussion

In this study, the augmentation of heat transfer in a differentially heated square enclosure filled with nanofluid was investigated. The nanofluid consists of TH29 PCM and nanoparticles with various volume fractions of  $\phi = 0, 0.1, \text{ and } 0.2$ . The accuracy of the present numerical method was verified by comparing with the results by Khodadadi and Hosseinizadeh [10]. As shown in fig. 2, the present solidification fronts are almost identical with those by Khodadadi and Hosseinizadeh with  $\phi = 0$  at various time steps. The maximum error is less than 2%. In addition, the grid dependency of solution was checked in fig. 3 by comparing the solidification fronts. The solution is almost unchanged after  $150 \times 150$ . However, in the present study, all the computations have been performed with  $200 \times 200$  grid system.

Figure 4 shows temporal evolution of PCM solidification front without particle, *i. e.*  $\phi = 0$ . As time goes by, the convective heat transfer starts to be prominent as thermal boundary layer thickness overcomes the conductive heat transfer. Just after the freezing process, the rate of solidification becomes considerable high because the cold wall absorbs the large amount of heat from the liquid. With increase in time, the propagation of solidification front becomes slower. Such difference causes the buoyancy force enabling the fluid flow to circulate in counterclockwise and the creation of thermal boundary layer near the solidification front. With further increase in time, the dominant heat transfer mode is changed as convection from conduction. The solid-liquid interface at bottom grows fast, and the convective region expands from the bottom of enclosure to the top. Since the Prandtl number is greater than one, the thermal boundary layer is thinner than the velocity boundary layer in the solidification front resulted from natural convection in liquid phase.

Figure 5 shows the temperature profiles and velocity streamlines at the early stage of solidification ( $t = 4.18 \cdot 10^4 \text{ s}$ ) for  $\phi = 0.1$ . The temperature appears uniform in the liquid side while it gradually

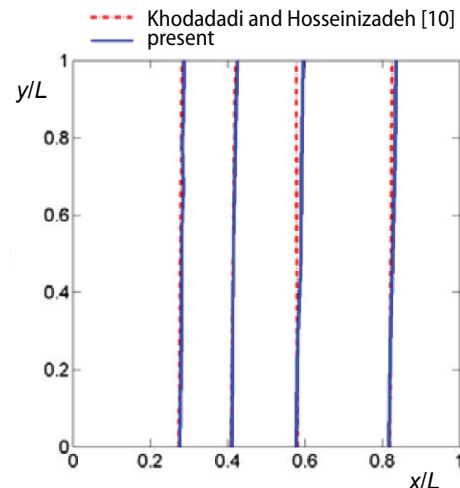


Figure 2. Comparison of solidification front

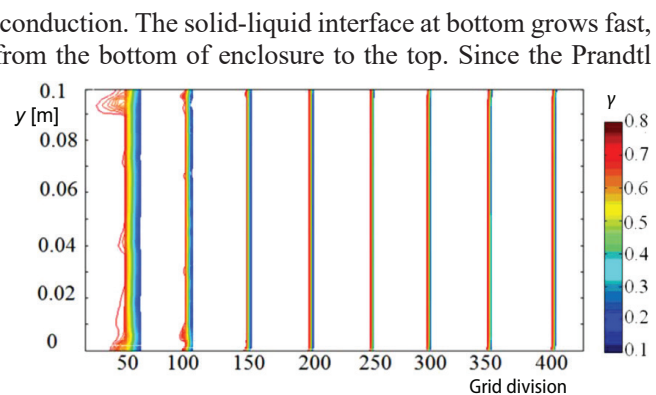


Figure 3. Phase change zone for various grid size

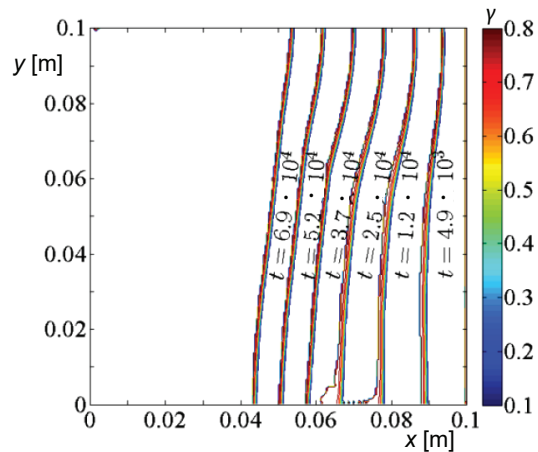


Figure 4. Variation of PCM solidification front with time for  $\phi = 0$

Figures 6 show the entropy generation in the enclosure. The entropy generation was computed by using the formula [32]:

$$S_{\text{gen}}^m = \frac{k_{\text{nf}}}{T^2} \left[ \left( \frac{\partial T}{\partial x} \right)^2 + \left( \frac{\partial T}{\partial y} \right)^2 \right] + \frac{\mu_{\text{nf}}}{T} \left[ 2 \left( \frac{\partial u}{\partial x} \right)^2 + 2 \left( \frac{\partial v}{\partial y} \right)^2 + \left( \frac{\partial u}{\partial y} + \frac{\partial v}{\partial x} \right)^2 \right] \quad (17)$$

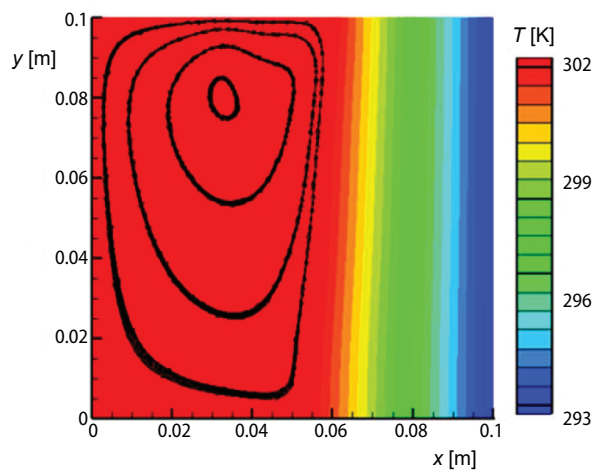


Figure 5. Temperature contour and velocity streamline at  $t = 4.18 \times 10^4$  s for  $\phi = 0.1$

decreases in solid phase. Noticeably, a flow circulation is found in liquid region. At  $t = 0$ , the temperature of the right boundary surface is suddenly lowered as  $T_c = T_m - \Delta T$  and this condition is maintained until the end of simulation. Thus, the solidification starts from the right surface with forming a solid-liquid interface and the front moves toward the negative x-direction. Here, the Stefan number defined as  $Ste = C_p \Delta T / H_{sf}$  expressing the significance of sensible heat relative to latent heat is less than approximately 0.1 and the heat exchange at the interface during phase change is little affected by the change of sensible enthalpy of the material during the heat transfer through the medium.

The most entropy generation occurs at the right solid region while the generation in the left liquid region is negligible because the significant temperature variation happens in the solid side. As shown in fig. 7, the most of the vortices produced near the top wall in liquid side where both the viscous heating and entropy generation is maximized. Note that the vorticity in solid region is inconsiderable.

The Brownian effect on the liquid fraction on the isotherm with  $T = T_m$  during the process is presented in fig. 8. The Brownian velocity is a function of temperature of liquid phase only, and it becomes slower near the solidification front whose the temperature is low. Also, the increase in thermal conductivity due to the Brownian motion expressed as the factor of

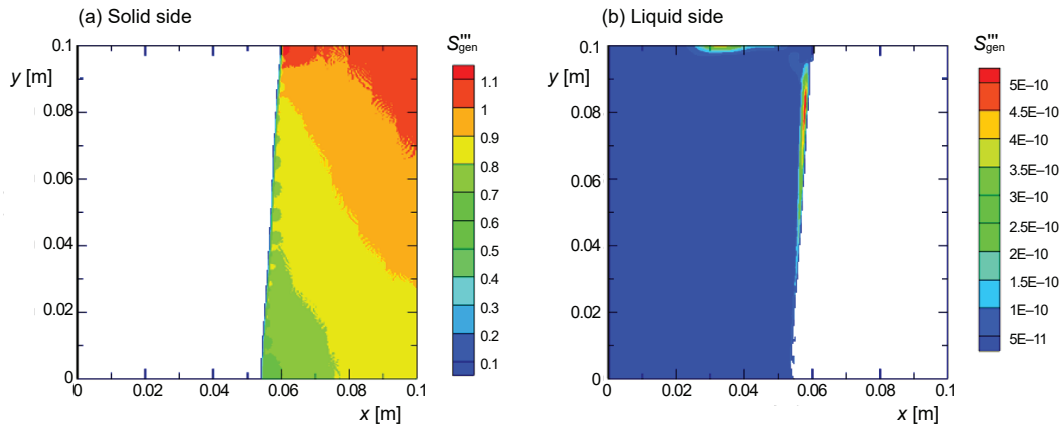


Figure 6. Entropy generation contour and velocity streamline at  $t = 4.18 \times 10^4$  s for  $\phi = 0.1$ ; (a) solid side, (b) liquid side

$$\left[ 1 + A(\text{Re}_p)^m \text{Pr}^{0.333} \phi \right]$$

in eq. (9) becomes smaller there. It should be noted however that the Brownian effect still enhances the thermal conductivity. Hence, with inclusion of Brownian effect, the total solidification time defined as the time required for the whole region in enclosure to be solidified, decrease as  $2.4339, 1.6541(\cdot 10^5$  s) from  $2.8446, 1.7801(\cdot 10^5$  s) for the nanofluid with  $\phi = 0.1$  and for the nanofluid with  $\phi = 0.2$ , respectively. The solidification time reduces by 35% with increase by the factor of 0.1 in  $\phi$  because the nanoparticles augmented the conduction and convection in the nanofluid, *i. e.* thermal conductivity and the natural convective heat transfer coefficient.

### Conclusions and recommendation

In this study, we have thoroughly examined the effects of nanoparticles on the unsteady phase change phenomena in a rectangular enclosure. The main results can be summarized as follows.

- The nanoparticles enhance the conduction through medium by its high thermal conductivity and enhance the convection by increasing the rate of phase change.
- In the phase change phenomena, the convective heat transfer becomes dominate over the conductive heat transfer as time goes by and. The nanoparticles accelerate such transition.

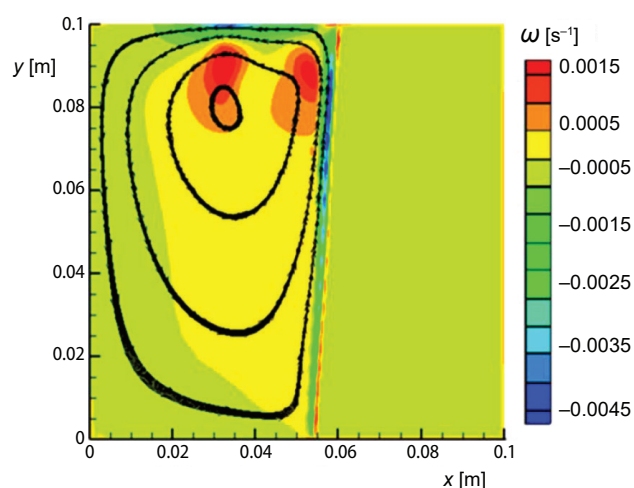


Figure 7. Vorticity at  $t = 4.18 \times 10^4$  s for  $\phi = 0.1$

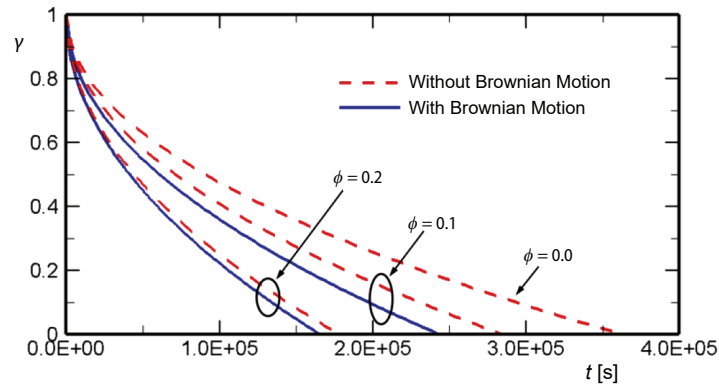


Figure 8. Liquid fraction versus time

- The energy capacity (or, thermal inertia) of the nanofluid (PCM with nanoparticles) is smaller than that of typical phase change materials.
- The PCM and nanoparticle mixed nanofluid can be used to regulate the medium temperature by control the balance between the solidification acceleration by nanoparticles and slowing-down by PCM.
- With consideration of the Brownian motion, the rate of phase change process increases, i.e. small total solidification time.

### Nomenclature

$C_p$  – specific heat capacity, [ $\text{Jkg}^{-1}\text{K}^{-1}$ ]  
 $g$  – gravity, [ $\text{ms}^{-2}$ ]  
 $H_{sf}$  – latent heat of melting, [ $\text{Jkg}^{-1}$ ]  
 $k$  – thermal conductivity, [ $\text{Wm}^{-1}\text{K}^{-1}$ ]  
 $P$  – pressure, [Pa]  
 $T$  – temperature, [K]  
 $u, v$  – x- and y-velocity, [ $\text{ms}^{-1}$ ]

### Greek symbols

$\beta$  – thermal expansion coefficient, [ $\text{K}^{-1}$ ]  
 $\gamma$  – liquid fraction, [–]

$\rho$  – density, [ $\text{kgm}^{-3}$ ]  
 $\phi$  – volume fraction of solid particles, [–]

### Subscripts

f – base fluid  
 l – liquid phase  
 m – freezing condition  
 nf – nanofluid  
 p – phase change material  
 ref – initial condition  
 s – solid phase

### Acknowledgment

This research was supported by Basic Science Research Program through the National Research Foundation of Korea (NRF) funded by the Ministry of Education, Science and Technology (NRF-2012R1A1A1042920).

### References

- [1] Kenisarin, M., Mahkamov, K., Solar Energy Storage Using Phase Change Materials. *Renewable and Sustainable Energy Reviews*, 11 (2007) 9, pp. 1913-1965
- [2] Omer, A., Renewable Building Energy Systems and Passive Human Comfort Solutions. *Renewable and Sustainable Energy Reviews*, 12 (2008) 6, pp. 1562-1587
- [3] Mehling, H., Cabeza, L. F., *Heat and Cold Storage with PCM*, Springer-Verlag, Heidelberg, Germany, 2008
- [4] Das, S. K., et al., *Nanofluids: Science and Technology*, John Wiley & Sons, New York, USA, 2007
- [5] Davis, S. H., *Theory of Solidification*, Cambridge University Press, Cambridge, UK, 2001
- [6] Maxwell, J. C., *A Treatise on Electricity and Magnetism*, Vol. 3, Dover, Mineola, New York, USA, 1954

- [7] Masuda, H., et al., Alteration of Thermal Conductivity and Viscosity of Liquid by Dispersing Ultra-Fine Particles, *Netsu Bussei*, 7 (1993), 4, pp. 227-233
- [8] Choi, U. S., Enhancing Thermal Conductivity of Fluids with Nanoparticles, in: *Developments and Application of Non-Newtonian Flow*, ASME, FED-Vol. 231/MD-V 66 (1995), pp. 99-105
- [9] Ho, C. J., et al., Thermophysical Properties of Nanoparticle-in-Paraffin Emulsion as Phase Change Material, *International Communications in Heat and Mass Transfer*, 36 (2009), 5, pp. 467-470
- [10] Khodadadi, J. M., Hosseinizadeh, F., Nanoparticle-Enhanced Phase Change Materials (NEPCM) with Great Potential for Improved Thermal Energy Storage, *International Communications in Heat and Mass Transfer*, 34 (2007), 5, pp. 534-543
- [11] Ranjbar, A. A., et al., Numerical Performance Study of Paraffin Wax Dispersed with Alumina in a Concentric Pipe Latent Heat Storage System. *Thermal Science*, 15 (2011), 1, pp. 169-181
- [12] Valan Arasu, A. et al., Numerical Heat Transfer Studies of a Latent Heat Storage System Containing Nano-Enhanced Phase Change Material, *Thermal Science*, 17 (2013), 2, pp. 419-430
- [13] Dutil, Y. et al., A Review on Phase-Change Materials: Mathematical Modeling and Simulations, *Renewable and Sustainable Energy Reviews*, 15 (2011), 1, pp. 112-130
- [14] Liu, S. et al., Mathematical Solutions and Numerical Models Employed for the Investigations of PCMs' Phase Transformations, *Renewable and Sustainable Energy Reviews*, 33 (2014), May, pp. 659-674
- [15] Qiu, L., et al., Experimental Research of PCMs – TH29 Using on Building Energy Storage, *Advanced Materials Research*, 569 (2012), Sep., pp. 202-206
- [16] Evers, A. C., Development of a Quantitative Measure of the Functionality of Frame Walls Enhanced with Phase Change Materials Using a Dynamic Wall Simulator, M. Sc. thesis, University of Kansas, Lawrence, Kans., USA, 2008
- [17] Assis, E., et al., Numerical and Experimental Study of Solidification in a Spherical Shell. *ASME Journal of Heat Transfer*, 131 (2009), 2, ID024502
- [18] Belhamadia, Y., et al., An Enhanced Mathematical Model for Phase Change Model for Phase Change Problems with Natural Convection. *International Journal of Numerical Analysis and Modeling, Series B*, 3 (2012), 2, pp. 192-206
- [19] Buyruk, E., et al., Numerical Investigation for Solidification around Various Cylinder Geometries. *Journal of Scientific & Industrial Research*, 68 (2009), 2, pp. 122-129
- [20] Kashani, S., et al., Numerical Analysis of Melting of Nanoparticle Enhanced Phase Change Material in Latent Heat Thermal Energy Storage System. *Thermal Science*, 18 (2014), Suppl. 2, pp. S335-S345
- [21] Batchelor, G., The Effect of Brownian Motion on the Bulk Stress in a Suspension of Spherical Particles, *Journal of Fluid Mechanics*, 83 (1977), 1, pp. 97-117
- [22] Hinch, J., A Perspective of Batchelor's Research in Micro-Hydrodynamics. *Journal of Fluid Mechanics*, 63 (2010), 6, pp. 8-17
- [23] Pan W., et al., Rheology, Microstructure and Migration in Brownian Colloidal Suspensions. *Langmuir* 26 (2010), 1, pp. 133-142
- [24] Einstein, A., *Investigation on the Theory of the Brownian Movement*, Dover, Mineola, New York, USA, 1956
- [25] Prasher, R., Thermal Conductivity of Nanoscale Colloidal Solutions (Nanofluids), *Physical Review Letters*, 94 (2005), Jan., ID025901
- [26] Nan, C.-W., et al., Effective Thermal Conductivity of Particulate Composites with Interfacial Thermal Resistance, *Journal of Applied Physics*, 81 (1997), 10, pp. 6692-6699
- [27] Lei, Q. M., Trupp, A. C., Experimental Study of Laminar Mixed Convection in the Entrance Region of a Horizontal Semicircular Duct, *International Journal of Heat and Mass Transfer*, 34 (1991), 9, pp. 2361-2372
- [28] Patankar, S. V., *Numerical Heat Transfer and Fluid Flow*, CRC Press, Boca Raton, Fla., USA, 1980
- [29] Chen, Y., Flaconer, R. A., Advection-Diffusion Modeling Using the Modified QUICK Scheme, *International Journal for Numerical Methods in Fluids*, 15 (1992), 10, pp. 1171-1191
- [30] Rhie, C. M., Chow, W. L., Numerical Study of Turbulent Flow Past an Airfoil with Trailing Edge Separation. *AIAA Journal*, 21 (1983), 11, pp. 1525-1532
- [31] \*\*\*, FLUENT 6.1 Manual
- [32] Bejan, A., *Entropy Generation Minimization*, CRC Press, Boca Raton, Fla., USA, 1996

Paper submitted: April 13, 2014

Paper revised: July 13, 2014

Paper accepted: July 14, 2014